Undergraduate Journal of Experimental Microbiology and Immunology (UJEMI) Vol. 27:1-11

Establishing a J774A.1 Murine Macrophage NLRP3 Inflammasome Model for Examining Short-Chain Fatty Acid Suppression

Samantha Cortez, Jerry He, Vince Lising

Department of Microbiology and Immunology, University of British Columbia, Vancouver, British Columbia, Canada

SUMMARY The NLRP3 inflammasome is an assembly of effector and adaptor proteins that mediates the release of pro-inflammatory cytokines, making it a key component of inflammation. While the inflammasome plays essential roles in pathogen clearance and homeostasis, it has also been linked to inflammatory diseases such as diabetes. With the increasing prevalence of obesity and type 2 diabetes, the inflammasome acts as a promising target for potential therapeutics. Recent studies have pointed to the role short-chain fatty acids might have in suppressing inflammation and the inflammasome. In this study, we set out to confirm whether the short-chain fatty acid, butyrate, has a suppressive effect on the NLRP3 inflammasome. We observed priming of the inflammasome in LPS-primed, ATP-activated J774A.1 macrophages through increased pro-IL-1β. However, mature IL-1β after ATP stimulation was not detected in our western blot analyses. Our cell viability and LDH cytotoxicity assays confirm ATP activation of the inflammasome through pyroptosis and LDH release. The establishment of a working NLRP3 model for J774A.1 macrophages will allow for research on the suppressive effects of short-chain fatty acids on the inflammasome and provide new avenues for potential therapeutics for inflammatory diseases such as diabetes.

INTRODUCTION

Obesity and type 2 diabetes have become increasingly prevalent in the past several decades. Since 1980, obesity rates in America have more than doubled, with 69% of adults presenting as obese or overweight in 2010; whereas in Canada, obesity rates have risen from 14% in 1979 to 25% in 2008 (1). Although rates have steadied since 2010, some models estimate that approximately half of the adult American population will classify as obese or overweight by the year 2030 (2). Interestingly, a large proportion of obesity cases are present alongside the diagnosis of type 2 diabetes. Type 2 diabetes affects approximately 10% of the Canadian and American populations, with an additional estimated 23% of adults being undiagnosed (3–5). A clear link between obesity and type 2 diabetes has been previously studied. While poor diet and lack of exercise have long been thought of as primary risk factors, research has begun to shed light on the role of chronic inflammation in the progression of these diseases (6–8). In fact, excess nutrient intake in obesity has been linked directly to adipose tissue remodeling, inflammasome activation, inflammation, and ultimately, impairment of the insulin signaling pathways and insulin resistance (7, 9). The NLRP3 inflammasome is a key culprit in the mediation of this inflammatory process (7, 8).

The NLRP3 (NOD-, LRR-, pyrin-domain containing protein 3) inflammasome is a multimeric assembly of effector and adaptor proteins that, upon activation, induces secretion of the pro-inflammatory cytokines IL-18 and IL-1β (10). As a key contributor to the innate immune response, NLRP3 is highly expressed in myeloid cells, including macrophages and dendritic cells, and is activated against a broad range of intracellular, extracellular, and environmental signals (10, 11). It comprises three major components: the NLRP3 sensor, ASC adapter, and caspase-1 effector. Upon activation, these components oligomerize to induce caspase-1 activation, pro-IL-1β and pro-IL-18 processing and their eventual secretion (10).

Published Online: September 2022

Citation: Samantha Cortez, Jerry He, Vince Lising. 2022. Establishing a J774A.1 Murine Macrophage NLRP3 Inflammasome Model for Examining Short-Chain Fatty Acid Suppression. UJEMI 27:1-11

Editor: Andy An and Gara Dexter, University of British Columbia

Address correspondence to: https://jemi.microbiology.ubc.ca/

NLRP3 inflammasome activation is a two-step process consisting of priming followed by activation. Priming is often facilitated by pathogen-associated molecular patterns (PAMPs), such as lipopolysaccharides (LPS) or damage-associated molecular patterns (DAMPs). The priming step serves as a signal to upregulate the inflammasome components NLRP3, caspase-1, and pro-IL-1β (10). The second step (activation), is caused by a broad suite of unrelated stimuli, including ATP, ion efflux, mitochondrial reactive oxygen species (ROS), and metabolic changes, leading to the oligomerization of the inflammasome, caspase-1 activation, and pro-inflammatory cytokine release (10, 12). NLRP3 activation also leads to pyroptosis, an inflammatory form of programmed cell death, characterized by excessive membrane bubbling and lactate dehydrogenase (LDH) release (10). Despite its considerable ability to induce inflammation, the NLRP3 inflammasome has been shown to be a largely redundant component of the innate immune system, as it functions in conjunction with a number of other inflammasomes, including NLRC4 and AIM2 (13).

The redundancy of NLRP3 signaling, coupled with emerging evidence of the detrimental role of NLRP3 in metabolic syndromes (including obesity and type 2 diabetes), has highlighted the importance of investigating the metabolic factors that regulate NLRP3 activation. While certain metabolic regulators of NLRP3 have been described, research into the role of lipid metabolism on NLRP3 activation requires deeper investigation (11). Previously, the fatty acid palmitate, a prevalent compound in high-fat diets, has been shown to activate the NLRP3 inflammasome (14, 15). However, the effects of other components of lipid metabolism on NLRP3 activation remain poorly described. One such example is the role short-chain fatty acids (SCFAs) play in regulating NLRP3 activation.

SCFAs are primary fermentation products of the human gut microbiota, primarily during dietary fibre breakdown (16). In humans and mice, acetate, propionate, and butyrate are the predominant SCFAs and are detectable in the millimolar range (16). As SCFAs are incorporated during fatty acid oxidation and have proposed anti-inflammatory effects to attenuate the pathogenesis of inflammatory diseases such as inflammatory bowel diseases, obesity, and type 1 and 2 diabetes, they are an exciting candidate for the metabolic regulation of NLRP3 (17, 18).

Accordingly, the ketone body beta-hydroxybutyrate (BHB), which is structurally homologous to the SCFA butyrate, has been shown to suppress NLRP3 inflammasome activation in various activation models through the inhibition of K^+ efflux, pro-IL-1β processing, caspase-1 activation, ROSs, and NF-kB phosphorylation (14, 19, 20). However, conflicting reports have emerged regarding the roles of SCFAs in NLRP3 suppression. For example, one study showed that neither butyrate, acetate, nor acetoacetate (another ketone body) had any effect on NLRP3 inflammasome activation in ATP, urate crystal, and lipotoxic acid (LTA)-activated bone marrow-derived macrophages (BMDM) (14). Another study found that butyrate, but not propionate or acetate, actually inhibited pro-IL-1β processing and NLRP3 inflammasome formation in cholesterol crystal-activated endothelial EOMA cell lines, possibly through catalase upregulation and inhibiting NLRP3 redox signaling (16). Additionally, butyrate and propionate have been shown to upregulate the antioxidant genes *SOD2* and *CAT* in malignant and nonmalignant human colon tissue, concurrent with the reported effect of BHB on these genes (21). A more recent report described SCFA-mediated suppression of pro-IL-1β processing in a palmitate-activated BMDM model (15). As palmitate is known to activate the NLRP3 pathway, this finding suggests that SCFAs may have an immunosuppressive role in NLRP3 that is specific to activation trigger. Altogether, this finding may indicate important roles of metabolic regulation in NLRP3-implicated metabolic syndromes.

To resolve conflicting reports regarding the role of SCFAs in inflammasome suppression, we aimed to determine whether short-chain fatty acid, butyrate, and ketone body, BHB, can suppress the NLRP3 inflammasome upon activation. We hypothesized that ATP-activated NLRP3 in J774A.1 murine macrophages treated with the butyrate or BHB will result in accumulated quantities of mature IL-1β, decreased pyroptosis, and decreased quantities of released LDH, altogether indicating decreased NLRP3 inflammasome activation. To test this hypothesis, we investigated the activation and suppression of the NLRP3 inflammasome in LPS-primed, ATP- or palmitate-activated J774A.1 murine macrophages. We conducted Western blot analysis, cell viability, and LDH cytotoxicity assays on LPS-primed, ATP-

activated J774A.1 murine macrophages. Here, we showed that signal 1 priming of the NLRP3 inflammasome upregulates pro-IL-1β expression in our model and confirmed that J774A.1 cells undergo pyroptotic cell death upon ATP-activation. Finally, we propose a working ATP stimulation model in J774A.1 cells for future use. The development of a working NLRP3 inflammasome assay in J774A.1 macrophages could initiate research into SCFA suppression of NLRP3, and provide insight into potential therapeutic regulators of NLRP3 and future research onNLRP3 metabolic regulation.

METHODS AND MATERIALS

Cell culture and stimulation for NLRP3 inflammasome activation. J774A.1 murine macrophage cell lines were obtained from the Kronstad Lab at the University of British Columbia and cultured in Dulbecco's Modified Eagle Medium (DMEM; Sigma) with 10% fetal bovine serum (FBS) (Thermofisher, Cat# 10438026) and L-glutamine (Thermofisher, Cat# 35050061). Cells were incubated in 37°C 5% CO_2. To prepare for stimulation, 6-well plates were seeded with $5x10^5$ cells per well and incubated overnight. Cells were primed with 500 ng/ml LPS (Sigma, Cat# L4391) for 4 hours and activated with either 5 mM ATP (Sigma, Cat# A2383), pH adjusted to 7 using NaOH, for 30 minutes or 200 µM palmitate (Sigma, Cat# P9767) for 16 hours. Suppressive capacities of short-chain fatty acids (SCFAs) and BHB were examined through co-incubation of 10 mM BHB (Sigma, Cat# H6501) or 10 mM butyrate (Sigma, Cat# 303401) with ATP or palmitate.

Cell Lysis and SDS-PAGE. Samples were collected after stimulation and rinsed twice with phosphate-buffered saline (PBS). Cells were resuspended in 75 µl ice-cold lysis buffer (20 mM Tris, pH 8, 137 mM NaCl, 10% glycerol, 2 mM EDTA, 1% Triton X-100 supplemented with cOmplete, EDTA-free Protease Inhibitor Cocktail (Sigma, Cat# 11873580001)) and centrifuged for 15 minutes at 14,000 x g to remove cell debris from the corresponding supernatants. Lysates were stored at -20°C. Protein concentration was then determined using Pierce BCA Protein Assay Kit (ThermoFisher, Cat# 23225) using bovine serum albumin (BSA) standards. At least 20 µg of total protein mixed with 1X protein loading buffer (0.25 M Tris-HCl pH 6.8, 8% SDS, 30% glycerol, 0.02% Bromophenol Blue containing 0.3 M DTT) were heated to 90°C for 5 minutes and loaded onto 12% acrylamide gels. SDS-PAGE was run at 200V for approximately 45 minutes followed by overnight Western transfer to Hybond-P:PVDF membranes in Western transfer buffer at 30V, 4°C.

Western blot analysis. To visualize separated bands of total transferred protein, membranes were incubated with Ponceau S and rinsed in distilled H_2O. Membranes were blocked in 5% skim milk in Tris-Buffered Saline with 0.1% Tween 20 (TBS-T) for 1 hour. All steps were performed at room temperature. IL-1β detection was performed using a 1:1000 dilution of anti-IL-1β goat polyclonal primary antibody (R&D, Cat# AF-401-SP) in 1% skim milk in TBS-T followed by a 1:15000 dilution of goat IgG HRP-conjugated secondary antibody (R&D, Cat# HAF109) in 1% skim milk, TBS-T. β-actin detection was performed using 1:5000 dilution of anti-β-actin mouse monoclonal primary antibody (Sigma, Cat# A5316) in 1% skim milk, TBS-T followed by 1:15000 dilution of goat anti-mouse IgG (H+L) secondary antibody (Invitrogen, Cat# 31430) in 1% skim milk, TBS-T. Blots were developed using Pierce ECL Western Blotting Substrate (ThermoFisher, Cat# 32106) and visualized using a ChemiDoc MP Imaging System (BioRad). Densitometry analysis was then performed using the ImageJ analysis program.

Visualization of pyroptosis with phase contrast and fluorescence microscopy. To observe pyroptosis of J774A.1 cells, a cell viability assay was performed. J774A.1 cells were seeded at a density of 6.0 x 10^5 cells per well in 6-well plates and incubated overnight at 37°C, 5% CO_2. Cells were then stimulated with 500 ng/ml LPS for 4 hours followed by stimulation with 5 mM ATP for 1 and 24 hours and 200 µM palmitate for 16 hours, either alone or together with 10mM BHB. Cell morphology was then visualized and imaged using an inverted phase-contrast microscope equipped with a Zeiss ERc5s camera. NucGreen Dead 488 (ThermoFisher, Cat# R37109) stain was then added as per manufacturer instructions to

fluorescently visualize cell viability using fluorescence microscopy. All images were captured using the 40X objective. Fluorescence microscopy images were further processed using the ImageJ analysis program.

LDH cytotoxicity assay. LDH activity in supernatants of ATP-stimulated J774A.1 cells was determined using the CyQUANT LDH Cytotoxicity Assay (Thermo, Cat# C20300) following manufacturer instructions, and absorbance was measured using a microplate reader (EPOCH Microplate Spectrophotometer, BioTek). In this assay, LDH activity is characterized by an increase in absorbance at 490 nm, and absorbance at 680 nm was used as the reference wavelength. Briefly, the optimal cell number was first determined by seeding 96-well plates with serial dilutions of 0-10,000 cells onto two sets of triplicate wells. Maximum LDH release was measured by the addition of Triton X-100 lysis buffer onto one set of triplicate wells and spontaneous LDH release was measured through the addition of 10µl of dH_2O onto the second set of triplicate wells. LDH activity was determined by subtracting absorbance measurements at 680 nm from the 490 nm absorbance value. Next, LDH cytotoxicity after NLRP3 activation was measured. 5 x 10^3 J774A.1 cells were primed with 500 ng/ml LPS for 4 hours followed by stimulation with 5 mM ATP for 0.5, 1, 2, or 4 hours. Time-course stimulation was conducted in triplicate per time point and transferred to a 96-well flat bottomed plate. Percent cytotoxicity (% cytotoxicity) was used to determine the amount of LDH release relative to fully lysed cells and was calculated using the following equation:

$$\% \text{ Cytotoxicity} = \frac{\text{(Palmitate/ATP)-treated LDH activity - Spontaneous LDH activity}}{\text{Maximum LDH activity - Spontaneous LDH activity}}$$

RESULTS

LPS induced pro-IL-1β upregulation, but ATP activation did not produce detectable mature IL-1β.

To determine the effects of SCFAs and BHB on the NLRP3 inflammasome, we first aimed to establish a working NLRP3 inflammasome model in ATP and palmitate-activated J774A.1 cells. To accomplish this, we probed for the pro- and mature forms of IL-1β by performing a Western blot on lysates of LPS-primed, ATP-activated, and butyrate and BHB-suppressed J774A.1 cells (Fig. 1).

While the palmitate-activation model was stimulated alongside our ATP-activation model, we encountered issues relating to cell adherence in the former, leading to inconclusive results (Supplementary Fig. 1). We thus decided to focus on the ATP activation model moving forward. Compared to untreated cells, we found that pro-IL-1β (31 kDa) was noticeably enriched in all LPS-treated conditions (Fig. 1). However, mature IL-1β (17 kDa) was not detected in any LPS-primed and ATP- treated conditions (Fig. 1). Nonetheless, all cells treated with LPS showed expression of pro-IL-1β, consistent with our hypothesis (Fig. 1). Furthermore, LPS-primed, ATP-activated, BHB and butyrate-treated cells, in addition to lacking mature IL-1β expression, did not seem to display an increased accumulation of pro-IL-1β. Altogether, these results suggest that LPS induces pro-IL-1β upregulation and that signal 1 NLRP3 inflammasome priming is working in our J774A.1 cell model. However, since mature IL-1β was not detected after ATP stimulation, we cannot conclude whether butyrate has suppressive effects on NLRP3 activation.

Membrane bubbling was observed in LPS-primed, ATP-stimulated J774A.1 macrophages.

Despite not detecting mature IL-1β, we focused on downstream pathways and tested whether ATP can successfully induce signal 2 and induce pyroptosis. We used phase contrast microscopy to observe for pyroptosis of J774A.1 cells primed with LPS and activated with ATP. We then conducted a membrane integrity-based cell viability assay with NucGreen Dead 488. Using inverted phase-contrast microscopy, we observed a drastic difference in cell morphology in LPS and ATP conditions. Specifically, LPS priming of J774A.1 cells showed

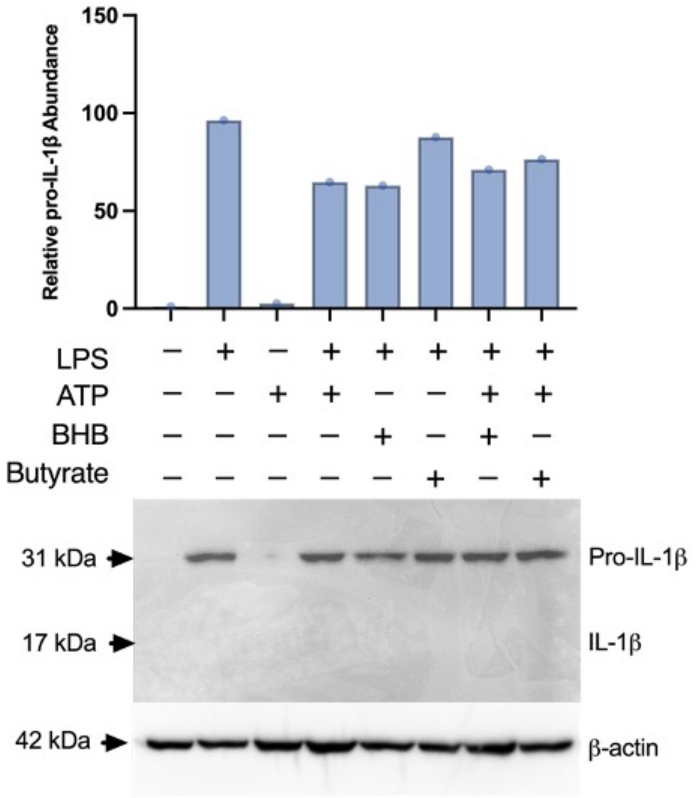

FIG. 1 Signal 1 priming of NLRP3 inflammasome induces pro-IL-1β expression. Western blot analysis of pro-IL-1β expression in J774A.1 cells treated with LPS (500 ng/ml; 4 hours) followed by stimulation with ATP (5 mM; 0.5 hour) in the presence of BHB (10 mM) or butyrate (10 mM). Bar graph represents pro-IL-1β band intensity obtained through densitometry analysis with ImageJ and normalized to β-actin and the negative control. n = 1.

an increase in filopodia (Fig. 2B), followed by a dramatic increase in membrane bubbling after 1 hour of ATP stimulation (Fig. 2C-D). In addition, fluorescence microscopy showed a substantial increase in cell death in the 24-hour ATP-treated conditions compared to 1-hour stimulation (Fig. 2K-L). However, we observed greater cell death in both 1 and 24-hour ATP-treated conditions compared to the unstimulated and LPS-only controls (Fig. 2E-G). Interestingly, the presence of BHB did not seem to have a suppressive effect on both the membrane bubbling morphology and viability seen in the ATP-activated cells, as cellular uptake of fluorescent dye was comparable to the LPS+ATP activated treatments (Fig. 2H, L). Overall, we were able to detect a working ATP-activation signal of the NLRP3 inflammasome through membrane bubbling and pyroptosis in J774A.1 cells.

Prolonged ATP stimulation in J774A.1 resulted in increased LDH activity.

Considering that signal 1 and signal 2 were likely functional in our NLRP3 model, we sought to quantitatively test signal 2 activation. In order to support our previous observation of pyroptosis (Fig. 2) and investigate the relationship between pyroptosis and ATP stimulation time, we performed an LDH cytotoxicity assay to measure LDH activity as a proxy for pyroptosis. To optimize the number of cells required to detect LDH activity while remaining in a linear relationship with absorbance, we measured LDH in increasing concentrations of J774A.1 cells (Fig. 3A). We ruptured the plasma membrane with lysis buffer to measure maximal LDH release and compared this to spontaneous release of LDH by the addition of water. With 2500 cells, we noticed detectable levels of LDH which increased linearly with absorbance at 5000 cells. However, beyond 5000 cells, absorbance no longer appeared to increase linearly, indicating that the assay was approaching the maximum detection limit (Fig. 3A).

Next, we conducted a time-course ATP-stimulation of J774A.1 cells to confirm the previous observation of pyroptosis (Fig. 2). Additionally, we sought to determine the optimal stimulation time where pyroptosis is detectable. Cells were stimulated with ATP at 0.5, 1, 2, and 4-hour time points and absorbances at 480 nm and 690 nm were measured to determine cytotoxicity. LDH activity was lowest at 0.5-hour stimulation and highest after 4-hour stimulation, indicating increased cytotoxicity with increased ATP stimulation time (Fig. 3B).

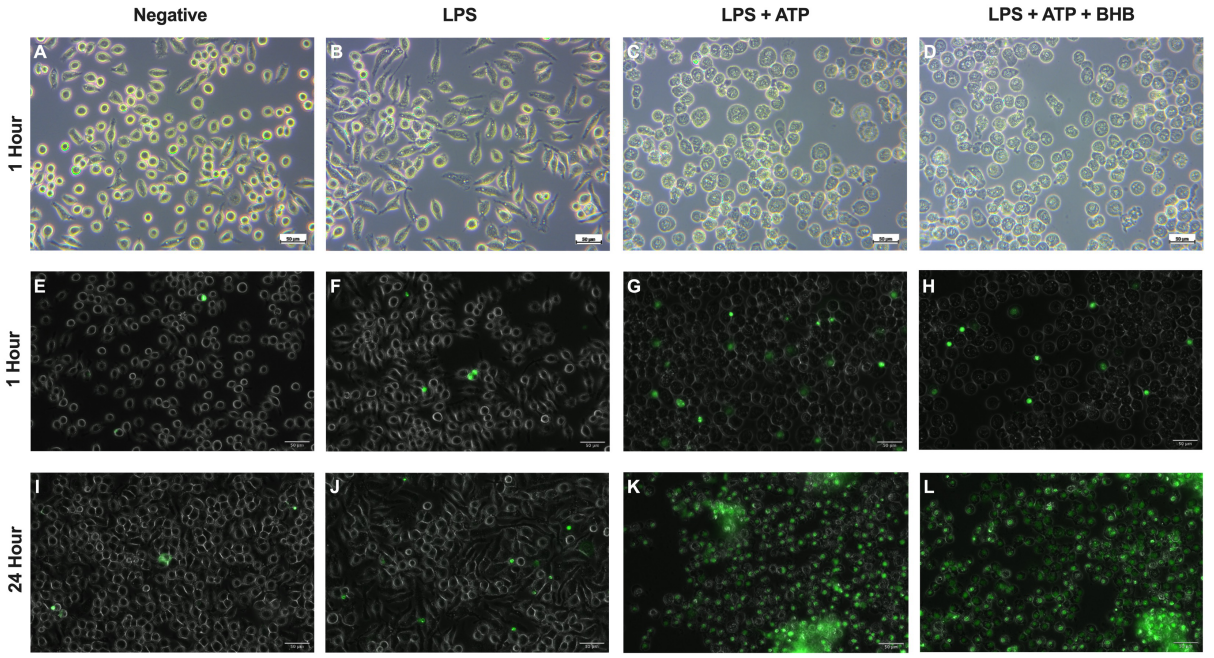

FIG. 2 Prolonged ATP stimulation of LPS-primed J774A.1 cells results in membrane bubbling and cell death (A-D) Phase-contrast images of J774A.1 cells after 500 ng/ml LPS priming for 4 hours and 5 mM ATP stimulation for 1 hour. **(E-L)** Epifluorescent microscopy images overlaid onto inverted-phase contrast images of the J774A.1 cells after 1 and 24-hour ATP stimulation stained with NucGreen Dead 488 (green) of the corresponding time points. Overlay images were generated using ImageJ. All images were obtained with 40X magnification.

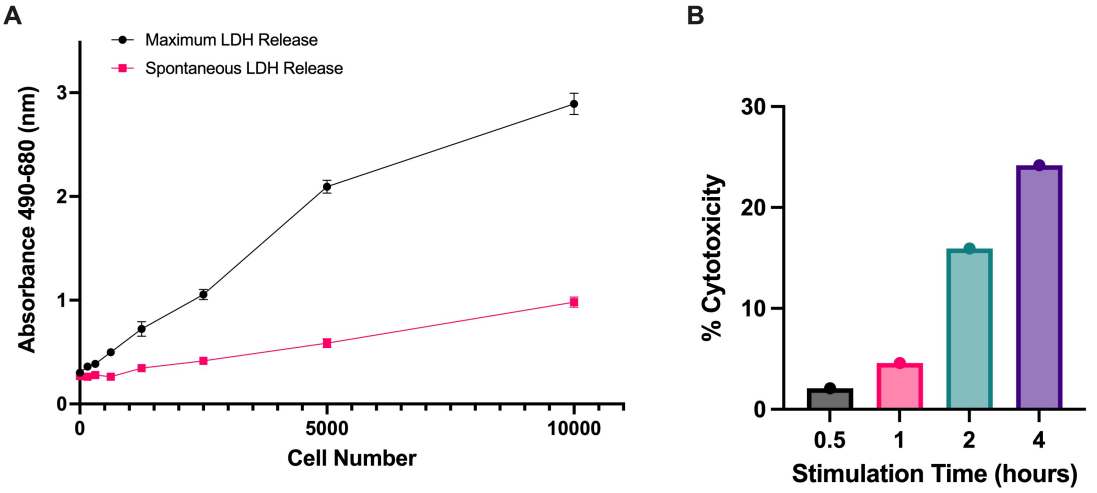

FIG. 3 Prolonged ATP stimulation leads to greater percent cytotoxicity. **(a)** Determination of optimal cell number for seeding J774A.1 murine macrophages and subsequent % cytotoxicity quantification. Maximum and spontaneous LDH release was determined through 45-minute incubation with Triton X-100 lysis buffer and dH_2O, respectively. **(b)** Percent cytotoxicity of J774A.1 cells after 4-hour LPS (500 ng/ml) priming followed by 0.5, 1, 2, or 4-hour ATP (5mM) stimulation in complete DMEM. LDH activity was determined through absorbance measurements at 490 nm and 680 nm. n = 1.

However, even after 2 and 4-hour treatments, only 16% and 25% cytotoxicity were observed (Fig. 3B). This could indicate that cells still had not fully undergone pyroptosis at this time (Fig. 3B). Indeed, these data provide evidence that a 30-minute stimulation may be insufficient to induce detectable cleavage of IL-1β in J774A.1 macrophages.

DISCUSSION

In this study, we aimed to determine whether the SCFA butyrate suppresses NLRP3 inflammasome activation in J774A.1 murine macrophages. While we were unable to detect mature IL-1β in our western blot analyses, we identified pro-IL-1β bands indicating successful priming with LPS in J774A.1 cells. We also observed LDH release and pyroptosis in our LDH cytotoxicity and cell viability assays, confirming ATP activation of the NLRP3 inflammasome.Ultimately, we were able to set up a foundation for an NLRP3 inflammasome model for examining short-chain fatty acid inhibition.

LPS activates signal 1 of the NLRP3 inflammasome and cell culture media may affect pro-IL-1β expression.

Through Western blot analysis of LPS-treated J774A.1 cells, we showed ~31 kDa bands corresponding to an upregulation of pro-IL-1β in all of our replicates, suggesting that LPS triggered signal 1 priming of the NLRP3 inflammasome pathway. Additionally, we identified the growth media RPMI 1640 + 10% FBS to be more effective at eliciting pro-IL-1β expression compared to complete DMEM, implying that J774A.1 cells may be more responsive to NLRP3 activation depending on the growth media of cells (Supplementary Fig. 2). Previous literature exploring the effect of growth media on cytokine gene expression in J774A.1 cells showed similar results, with LPS inducing more IL-1β expression in RPMI compared to DMEM (26). With this in mind, RPMI 1640 with 10% FBS supplementation may improve the likelihood of detecting secreted IL-1β in our model. However, we did not detect bands corresponding to mature IL-1β (Fig. 1). This unexpected result may have been caused by several factors. First, the ATP concentrations and stimulation times used (up to 5 mM; 30 minutes) may have been insufficient to induce cleavage of pro-IL-1β. Previous studies investigating NLRP3 inflammasome activation with ATP have opted to use stimulations times between 30-minutes and 1-hour, as well as ATP concentrations ranging from 0.5 mM to 5 mM in J774A.1 macrophages and bone marrow-derived macrophages (BMDMs) (14, 22–24). In fact, we determined that cell death was highest after 4 hours of 5 mM ATP stimulation indicating that longer ATP stimulation may be required to induce optimal pyroptosis and detect mature-IL-1β expression (Fig. 3B). Another possibility for the lack of mature IL-1β in our blots is that the amount of protein loaded onto the gel prior to antibody probing was too low. In our study, we analyzed 25 µg of total protein to assess IL-1β expression by Western blotting. However, another study using the same cell line with LPS-priming and ATP activation loaded 50 µg of cell lysate prior to Western blot analysis and achieved a high signal of mature IL-1β (25). Finally, we may not have detected mature IL-1β in our Western blots due to our focus on analyzing cell lysates instead of cell supernatants. Interestingly, another study that performed Western blots on both cell lysates and supernatants of LPS-primed, ATP-activated J774A.1 cells showed stronger IL-1β signals in the latter approach (24), which supports the possibility that mature IL-1β is more abundant in the cell culture supernatant.

Overall, we demonstrated that LPS-primed J774A.1 cells have a working signal 1 and show a greater expression of pro-IL-1β in RPMI 1640 with 10% FBS compared to DMEMc. However, because of the lack of visible mature IL-1β after ATP stimulation, we are restricted from making conclusions regarding the suppressive effects of both BHB and butyrate.

J774A.1 murine macrophages release LDH and undergo pyroptosis after ATP-mediated NLRP3 inflammasome activation.

To confirm whether signal 2 activation of the NLRP3 inflammasome with ATP is working in our model, we conducted a visual cell viability assay on LPS-primed, ATP-activated J774A.1 cells. Indeed, membrane bubbling and decreased membrane integrity were observed as early as 1-hour post ATP stimulation with increased cell death after 24 hours (Fig. 2). The observed morphology change and cell death likely suggest pyroptosis, a pro-inflammatory form of cell death and a known outcome of NLRP3 inflammasome activation (28). As Zha *et al.* have shown that ATP can induce pyroptosis, prolonged ATP exposure could explain the rise in cell death seen in 24-hour stimulation conditions as compared to 1 hour ATP stimulation (24). Additionally, membrane bubbling is not indicative of cell death as the membrane integrity of these cells remain intact, excluding the fluorescent dye (30).

This likely explains why cell death was not widely observed in 1 hour ATP stimulation. While we were not able to detect ATP-dependent cleavage of IL-1β in our Western blot analyses, we did observe the prototypical expansion of the plasma membrane (membrane bubbling) and LDH release, suggesting that NLRP3 activation and induction of pyroptosis had occurred in our cells in response to ATP. However, ATP concentrations and stimulation times likely need to be optimized in order to detect mature IL-1β in Western blots.

ATP stimulation times of 4h may be ideal for the detection of cleaved IL-1β.

Through an LDH cytotoxicity assay, we determined that LDH activity increased drastically between 0.5 to 4 hours of ATP stimulation. 4-hour ATP stimulation appeared to induce 4 times more LDH activity than the 0.5-hour treatment with even a 1-hour treatment resulting in doubled LDH activity. We argue that 0.5-hour stimulation with 5mM ATP may not be sufficient to detect mature IL-1β, which may explain why we could not detect appreciable levels in our Western Blots (Fig. 1). Instead, prolonged stimulation of 1 or more hours may be optimal for detection. One challenge in determining an optimal ATP stimulation time is to ensure that the cells do not undergo pyroptosis significantly prior to collecting cell lysates. Considering that LPS-primed, ATP-activated J774A.1 cells only released 25% LDH compared to maximally lysed cells, a stimulation time of 4 hours may be more appropriate for the detection of mature IL-1β. Indeed, as mentioned previously, there is a range of ATP stimulation times reported for NLRP3 inflammasome activation (14, 22–24). We thus conclude that a 0.5 hr ATP stimulation (2% LDH activity) is insufficient to detect IL-1β cleavage in our model.

Proposing a working model for NLRP3 inflammasome activation in J774A.1 murine macrophages

We demonstrate a working signal 1 priming step in J774A.1 murine macrophages, inducing upregulation of pro-IL-1β. However, we were unable to detect mature IL-1β and confirm successful signal 2 activation of our NLRP3 inflammasome model with either ATP or palmitate activators. Microscopy and LDH activity assays, however, support the notion that ATP activates the NLRP3 inflammasome as pyroptosis was observable 1 hour post-treatment and LDH release increased with time post-treatment. Moreover, our data suggest that a 0.5-hour ATP stimulation is insufficient to detect mature IL-1β. Thus, we would like to propose a possible working ATP stimulation model of the NLRP3 inflammasome in J774A.1 cells. In this model, J774A.1 cells should be grown to >90% confluency in 6-well plates with RPMI 1640 + 10% FBS media (Supplementary Fig. 1). The NLRP3 inflammasome can be primed with 500 ng/ml LPS for 4 hours followed by signal 2 stimulation with 5mM ATP for >1 hour. Cells should be lysed with 50 to 75ul of Triton X-100 lysis buffer and ~30-50 μg of protein should be loaded onto a polyacrylamide gel for western blotting. If ~30-50 μg of protein is unobtainable through regular cell lysis, we propose that the lysates either be concentrated with a low molecular weight cut-off (1-5 kDa) centrifugal ultrafiltration device or that protein be precipitated out of the lysate using a precipitant such as ammonium sulfate (33). Following this model, we believe that mature IL-1β will be detectable via Western blots of J774A.1 cell lysates.

Limitations While our microscopy for cell viability (Fig. 2) and LDH cytotoxicity assay (Fig. 3) implied pyroptosis and NLRP3 activation, a major limitation was our inability to establish signal 2 activation of NLRP3 in our Western blot procedures. Since the literature strongly supports ATP as a potent activator of NLRP3, this finding suggests an issue with the proper functioning of our model (28). Furthermore, without a working positive control for cleavage of pro-IL-1β, we are restricted from making conclusions regarding the BHB and butyrate-mediated suppression of the NLRP3 inflammasome, leaving our major research question unanswered.

Another limitation was having to exclude the use of palmitate to induce inflammasome activation, since in our hands, palmitate treatment led to cell detachment. We were interested in this model because it has been shown that SCFAs can suppress palmitate-dependent NLRP3 inflammasome activation in BMDMs.

(14, 36). Thus, it would be interesting to determine whether palmitate-activated cells are similarly prone to NLRP3 suppression in our J774A.1 cell model. However, we observed that palmitate-treated cells consistently detached from the well surface compared to untreated, LPS only-treated, and ATP-treated cells, preventing us from drawing reliable conclusions for palmitate treatments in all of our experiments.

Additionally, our LDH cytotoxicity assay lacked proper LPS and ATP-only controls. Therefore, our study is limited in the sense that we are not able to accurately compare LDH release between the LPS and ATP-only conditions and the LPS+ATP treated cells. Future studies should pilot a working assay with LPS and ATP-only controls.

Finally, our exclusive use of antibodies against IL-1β as a proxy for NLRP3 inflammasome activation in our Western blot analyses heavily constricts our findings. Since the NLRP3 inflammasome is a complex formation, probing for other components, such as caspase-1, would strengthen our argument for NLRP3 activation. In fact, other studies on the same topic use a multitude of antibody probes to corroborate their findings (14, 22–24). Additionally, it is possible that some components of the NLRP3 inflammasome are more highly expressed than others, which would allow for a better chance of detecting a signal (28).

Conclusions The aim of our study was to determine whether the SCFA, butyrate, is able to suppress NLRP3 inflammasome activation. Overall, western blot analysis showed a working signal 1 LPS priming of the inflammasome but has yet to detect mature IL-1β to confirm signal 2 activation with ATP. However, time-course stimulation of ATP showed membrane bubbling and LDH release starting at 1 hour post-stimulation followed by total cell death at 24 hours, confirming that signal 2 activation is occurring in our cell models.

Future Directions Due to the lack of mature IL-1β shown in our Western blots, confirmation of signal 2 inflammasome activation, which induces cleavage of pro-IL-1β, is a crucial next step in refining our NLRP3 inflammasome model. Specifically, it would be useful to perform a time course stimulation with varying ATP concentrations to determine the optimal ATP condition where cleaved IL-1β is visible. Of note, our ATP stimulation time for our Western blot did not exceed one hour, whereas previous studies have observed pro-IL-1β cleavage at longer stimulation times (14, 22–24). Another option is to increase the concentration of ATP, or to use a variety of different activators such as uric acid or nigericin, to see if mature IL-1β expression in this cell line is dependent on the specific signal 2 activator. Finally, increasing the protein loading amount for western blot analysis could potentially resolve the uncertainty of whether the protein amount loaded in our procedure was insufficient for detection. These approaches would help elucidate the reason why mature IL-1β was not detected in our western blots and would be beneficial in refining our proposed model.

Our experiments primarily consisted of Western blots on cell lysates of J774A.1 cells. However, we suggest performing similar treatments using a more quantitative approach such as an enzyme-linked immunosorbent assay (ELISA). ELISAs are commonly used to study NLRP3 activation in various inflammasome models (37). The high specificity of an ELISA coupled with an antibody specific for mature IL-1β may be sufficient to detect the secreted cytokine more efficiently than Western blotting. Additionally, this technique can be easily performed on cell culture supernatants, which may possibly contain more secreted mature IL-1β than in cell lysates (38). Altogether, the use of an ELISA could work effectively to corroborate our results.

Overall, these approaches will help to establish a detectable signal 2 in our NLRP3 inflammasome model, which will allow future studies to test whether SCFAs such as butyrate have suppressive effects on NLRP3.

ACKNOWLEDGEMENTS

We would like to give a special thank you to Dr. Marcia Graves and Ameena Hashimi for providing valuable guidance throughout our project. We would also like to give a thank you to our fellow MICB 421 classmates for their tremendous support along the way and the lab

staff for the maintenance and upkeep of lab resources and equipment. Lastly, we would like to show appreciation to the Department of Microbiology and Immunology at the University of British Columbia for providing funding and resources for this project.

CONTRIBUTIONS

This paper was a result of the collaborative effort of all authors. All authors equally contributed time for laboratory experiments and data acquisition. S.C. was responsible for data analysis and figure generation and writing the abstract and methods. J.H. was responsible for developing the initial project proposal and conducting background research. V.L. contributed data analyses and discussion points in the manuscript.

REFERENCES

1. Flegal KM, Carroll MD, Kit BK, Ogden CL. 2012. Prevalence of Obesity and Trends in the Distribution of Body Mass Index Among US Adults, 1999-2010. JAMA 307:491.
2. Harvard T.H. Chan School of Public Health. Adult Obesity. https://www.hsph.harvard.edu/obesity-prevention-source/obesity-trends/obesity-rates-worldwide/.
3. Hosseini Z, Whiting SJ, Vatanparast H. 2019. Type 2 diabetes prevalence among Canadian adults — dietary habits and sociodemographic risk factors. Appl Physiol Nutr Metab 44:1099–1104.
4. Centers for Disease Control and Prevention. 2022. National Diabetes Statistics Report. https://www.cdc.gov/diabetes/data/statistics-report/index.html.
5. Centers for Disease Control and Prevention. 2021. Diabetes and Obesity Maps. https://www.cdc.gov/diabetes/data/center/slides.html.
6. Esser N, Legrand-Poels S, Piette J, Scheen AJ, Paquot N. 2014. Inflammation as a link between obesity, metabolic syndrome and type 2 diabetes. Diabetes Res Clin Pract 105:141–150.
7. Wani K, AlHarthi H, Alghamdi A, Sabico S, Al-Daghri NM. 2021. Role of NLRP3 Inflammasome Activation in Obesity-Mediated Metabolic Disorders. Int J Environ Res Public Health 18:511.
8. Grant RW, Dixit VD. 2013. Mechanisms of disease: inflammasome activation and the development of type 2 diabetes. Front Immunol 4.
9. Wen H, Gris D, Lei Y, Jha S, Zhang L, Huang MT-H, Brickey WJ, Ting JP-Y. 2011. Fatty acid–induced NLRP3-ASC inflammasome activation interferes with insulin signaling. Nat Immunol 12:408–415.
10. Hughes MM, O'Neill LAJ. 2018. Metabolic regulation of NLRP3. Immunol Rev 281:88–98.
11. Swanson K V., Deng M, Ting JP-Y. 2019. The NLRP3 inflammasome: molecular activation and regulation to therapeutics. Nat Rev Immunol 19:477–489.
12. Zheng D, Liwinski T, Elinav E. 2020. Inflammasome activation and regulation: toward a better understanding of complex mechanisms. Cell Discov 6:36.
13. Coll R, O'Neill L, Schroder K. 2016. Questions and controversies in innate immune research: what is the physiological role of NLRP3? Cell Death Discov 2:16019.
14. Youm Y-H, Nguyen KY, Grant RW, Goldberg EL, Bodogai M, Kim D, D'Agostino D, Planavsky N, Lupfer C, Kanneganti TD, Kang S, Horvath TL, Fahmy TM, Crawford PA, Biragyn A, Alnemri E, Dixit VD. 2015. The ketone metabolite β-hydroxybutyrate blocks NLRP3 inflammasome–mediated inflammatory disease. Nat Med 21:263–269.
15. Truax AD, Chen L, Tam JW, Cheng N, Guo H, Koblansky AA, Chou W-C, Wilson JE, Brickey WJ, Petrucelli A, Liu R, Cooper DE, Koenigsknecht MJ, Young VB, Netea MG, Stienstra R, Sartor RB, Montgomery SA, Coleman RA, Ting JP-Y. 2018. The Inhibitory Innate Immune Sensor NLRP12 Maintains a Threshold against Obesity by Regulating Gut Microbiota Homeostasis. Cell Host Microbe 24:364-378.e6.
16. Yuan X, Wang L, Bhat OM, Lohner H, Li P-L. 2018. Differential effects of short chain fatty acids on endothelial Nlrp3 inflammasome activation and neointima formation: Antioxidant action of butyrate. Redox Biol 16:21–31.
17. Aoun A, Darwish F, Hamod N. 2020. The Influence of the Gut Microbiome on Obesity in Adults and the Role of Probiotics, Prebiotics, and Synbiotics for Weight Loss. Prev Nutr Food Sci 25:113–123.
18. Parada Venegas D, De la Fuente MK, Landskron G, González MJ, Quera R, Dijkstra G, Harmsen HJM, Faber KN, Hermoso MA. 2019. Short Chain Fatty Acids (SCFAs)-Mediated Gut Epithelial and Immune Regulation and Its Relevance for Inflammatory Bowel Diseases. Front Immunol 10.
19. Kong G, Huang Z, Ji W, Wang X, Liu J, Wu X, Huang Z, Li R, Zhu Q. 2017. The Ketone Metabolite β-Hydroxybutyrate Attenuates Oxidative Stress in Spinal Cord Injury by Suppression of Class I Histone Deacetylases. J Neurotrauma 34:2645–2655.
20. Traba J, Geiger SS, Kwarteng-Siaw M, Han K, Ra OH, Siegel RM, Gius D, Sack MN. 2017. Prolonged fasting suppresses mitochondrial NLRP3 inflammasome assembly and activation via SIRT3-mediated activation of superoxide dismutase 2. J Biol Chem 292:12153–12164.

21. Jahns F, Wilhelm A, Jablonowski N, Mothes H, Greulich KO, Glei M. 2015. Butyrate modulates antioxidant enzyme expression in malignant and non-malignant human colon tissues. Mol Carcinog 54:249–260.
22. Karmakar M, Katsnelson MA, Dubyak GR, Pearlman E. 2016. Neutrophil P2X7 receptors mediate NLRP3 inflammasome-dependent IL-1β secretion in response to ATP. Nat Commun 2016 71 7:1–13.
23. Zhong C, Wang R, Hua M, Zhang C, Han F, Xu M, Yang X, Li G, Hu X, Sun T, Ji C, Ma D. 2021. NLRP3 Inflammasome Promotes the Progression of Acute Myeloid Leukemia via IL-1β Pathway. Front Immunol 12:2113.
24. Zha QB, Wei HX, Li CG, Liang YD, Xu LH, Bai WJ, Pan H, He XH, Ouyang DY. 2016. ATP-induced inflammasome activation and pyroptosis is regulated by AMP-activated protein kinase in macrophages. Front Immunol 7:597.
25. Chiu HW, Li LH, Hsieh CY, Rao YK, Chen FH, Chen A, Ka SM, Hua KF. 2019. Glucosamine inhibits IL-1β expression by preserving mitochondrial integrity and disrupting assembly of the NLRP3 inflammasome. Sci Rep 9:1–13.
26. Wu CH, Gan CH, Li LH, Chang JC, Chen ST, Menon MP, Cheng SM, Yang SP, Ho CL, Chernikov O V., Lin CH, Lam Y, Hua KF. 2020. A Synthetic Small Molecule F240B Decreases NLRP3 Inflammasome Activation by Autophagy Induction. Front Immunol 11:3330.
27. Cohly H, Cohly H, Stephens J, Markhov A, Angel M, Campbell W, Ndebele K, Jenkins J. 2001. Cell culture conditions affect LPS inducibility of the inflammatory mediators in J774A.1 murine macrophages. Immunol Invest 30:1–15.
28. Kelley N, Jeltema D, Duan Y, He Y. 2019. The NLRP3 Inflammasome: An Overview of Mechanisms of Activation and Regulation. Int J Mol Sci 2019, Vol 20, Page 3328 20:3328.
29. Adeshakin FO, Adeshakin AO, Afolabi LO, Yan D, Zhang G, Wan X. 2021. Mechanisms for Modulating Anoikis Resistance in Cancer and the Relevance of Metabolic Reprogramming. Front Oncol 11:528.
30. Zhang Y, Chen X, Gueydan C, Han J. 2018. Plasma membrane changes during programmed cell deaths. Cell Res 28:9–21.
31. Ogawa Y, Imajo K, Honda Y, Kessoku T, Tomeno W, Kato S, Fujita K, Yoneda M, Saito S, Saigusa Y, Hyogo H, Sumida Y, Itoh Y, Eguchi K, Yamanaka T, Wada K, Nakajima A. 2018. Palmitate-induced lipotoxicity is crucial for the pathogenesis of nonalcoholic fatty liver disease in cooperation with gut-derived endotoxin. Sci Reports 2018 81 8:1–14.
32. Hetherington AM, Sawyez CG, Zilberman E, Stoianov AM, Robson DL, Borradaile NM. 2016. Differential Lipotoxic Effects of Palmitate and Oleate in Activated Human Hepatic Stellate Cells and Epithelial Hepatoma Cells. Cell Physiol Biochem 39:1648–1662.
33. Chen H, Ma J, Liu J, Dou L, Shen T, Zuo H, Xu F, Zhao L, Tang W, Man Y, Ma Y, Li J, Huang X. 2022. Lysophosphatidylcholine disrupts cell adhesion and induces anoikis in hepatocytes. FEBS Lett 596:510–525.
34. Han MS, Jung DY, Morel C, Lakhani SA, Kim JK, Flavell RA, Davis RJ. 2013. JNK expression by macrophages promotes obesity-induced insulin resistance and inflammation. Science 339:218–222.
35. Mallinson SJB, Machovina MM, Silveira RL, Garcia-Borràs M, Gallup N, Johnson CW, Allen MD, Skaf MS, Crowley MF, Neidle EL, Houk KN, Beckham GT, Dubois JL, McGeehan JE. 2018. A promiscuous cytochrome P450 aromatic O-demethylase for lignin bioconversion. Nat Commun 2018 91 9:1–12.
36. Truax AD, Chen L, Tam JW, Cheng N, Guo H, Koblansky AA, Chou WC, Wilson JE, Brickey WJ, Petrucelli A, Liu R, Cooper DE, Koenigsknecht MJ, Young VB, Netea MG, Stienstra R, Sartor RB, Montgomery SA, Coleman RA, Ting JPY. 2018. The Inhibitory Innate Immune Sensor NLRP12 Maintains a Threshold against Obesity by Regulating Gut Microbiota Homeostasis. Cell Host Microbe 24:364-378.e6.
37. Di Virgilio F, Pelegrín P, Riteau N, Gombault A, Couillin I. 2016. Assessment of Inflammasome Activation by Cytokine and Danger Signal Detection. Methods Mol Biol 1417:63–74.
38. Zhang X, Cheng Y, Xiong Y, Ye C, Zheng H, Sun H, Zhao H, Ren Z, Xu J. 2012. Enterohemorrhagic Escherichia coli Specific Enterohemolysin Induced IL-1β in Human Macrophages and EHEC-Induced IL-1β Required Activation of NLRP3 Inflammasome. PLoS One 7:e50288.